International Core Journal of Engineering Volume 11 Issue 6, 2025
ISSN: 2414-1895 DOI: 10.6919/ICJE.202506_11(6).0033

Real-Time Navigation Line Extraction for Cabbage Harvesting Robots in Complex Farmland Environments: A Multi-Mask Fusion and Dynamic Row-Tracking Approach

Jing Zhang[1,2,a], Yuan Ma[1,b], Yizhuo Fan[1,c], Nan Su[3,d], Xun He[1,e], and Hongmei Zhang[1,f,*]

[1] School of Mechanical and Electrical Engineering, Henan Agricultural University, Zhengzhou 450002, China

[2] Key Laboratory of on Site Processing Equipment for Agricultural Products, Ministry of Agriculture and Rural Affairs, Hangzhou 310058, China

[3] School of Information and Management Science (Software School), Henan Agricultural University, Zhengzhou 450002, China

[a]zj_xjau@vip.163.com, [b]1154438012@qq.com, [c]fanyizhuo123@yeah.net, [d]sunan@henau.edu.cn, [e]hexun876@163.com, [f,*]zhanghongmei0905@henau.edu.cn

Abstract

As an important leafy vegetable economic crop in China, cabbage harvesting is faced with problems such as low efficiency of manual operation, high labor intensity and high labor cost. However, the existing navigation technologies for harvesting robots has shortcomings in accuracy and adaptability to complex environments.This research presents an advanced navigation line extraction framework tailored for automated cabbage harvesting, targeting the challenges posed by mature heading-stage crops in diverse field conditions. By introducing a multi-mask fusion segmentation strategy grounded in the HSV color model, the study overcomes the limitations of conventional grayscale methods, enabling precise separation of cabbage vegetation and plastic mulch while effectively suppressing interference from weeds, soil reflections, and plant yellowing. Three key algorithmic innovations are developed: First, an adaptive row-tracking algorithm incorporates dynamic historical midpoint adjustment and perspective-constrained hierarchical scanning, achieving an average angular accuracy of 0.24° for central navigation lines across high- and low-light environments, with a 94% reduction in false edge detections compared to traditional sliding window techniques. Second, a RANSAC-based robust fitting method reduces boundary line extraction time to 0.192 seconds per frame and centerline fitting time to less than 0.001 seconds, demonstrating superior performance in handling complex scenarios such as missing plants, curved rows, and heading angle deviations up to 15°. Third, a vector bisector-based centerline extraction approach, utilizing geometric intersection modeling and direction vector synthesis, ensures navigation lines maintain an accuracy within 2 pixels relative to manual annotations. Experimental validation in Xiangcheng County, Henan Province, using the 'Zhonggan 56' cabbage variety, confirms the framework's effectiveness, achieving an average precision rate of 92% (defined as the ratio of correctly detected rows to total annotated rows) across varied field conditions including weedy plots and camera tilts. These findings establish a reliable foundation for automated cabbage harvesting systems, with potential applications extending to other leafy vegetable crops. Future research will focus on field deployment via edge computing,

ISSN: 2414-1895 DOI: 10.6919/ICJE.202506_11(6).0033

followed by algorithm optimization through parallel architectures and deep learning integration and GIS technologies for large-scale agricultural management.

Keywords

Cabbage; Crop Row Detection; Navigation Line Extraction; Computer Vision; Agricultural Automation.

1. Introduction

Cabbage (*Brassica oleracea L.*), a staple leafy vegetable crop in China, achieved a cultivation area exceeding 1.2 million hectares and an annual yield of 35 million tons in 2023. Traditional harvesting, however, remains highly labor-dependent, plagued by inefficiencies, high physical demands, and escalating costs. Manual picking takes over five seconds per head, limiting daily output to 0.2 - 0.3 hectares, while continuous bending raises lumbar injury risks by 3.2 times[1-3]. Labor expenses account for 40 - 60% of production costs, growing 8% - 10% annually [4-5]. In large-scale operations, these limitations hinder timely harvesting within critical 48-hour windows and render the process vulnerable to adverse weather conditions like rain-induced field mud.

Agricultural automation technologies offer potential remedies, yet existing cabbage harvesting robots face substantial hurdles[6-8]. Their navigation systems typically exhibit angular errors exceeding 8° and positioning deviations over 10 cm, while complex environments-characterized by dense foliage (over 60% canopy coverage) or extreme lighting gradients (above 2000 lux)-cause system failures in 25% of cases[9-10]. Achieving sub-5 cm positioning accuracy, 10 Hz update rates, and heading precision within ±3° is essential for effective automation.

Computer vision, renowned for non-invasive sensing and high-resolution data acquisition, presents a viable solution for agricultural navigation[11]. Advanced methods such as U-Net-based segmentation and point cloud matching enable accurate identification of crop rows, boundaries, and obstacles with 3D reconstruction errors under 8 cm. Nevertheless, cabbage cultivation poses unique visual challenges. Its dense canopies increase clustering errors by 18%, while spectral similarities between cabbage leaves and soil-with a color difference (ΔE) below the 20 units machine vision threshold-complicate segmentation[12-14]. Weed interference and uneven illumination further degrade traditional algorithms, reducing their success rates by 22% and 40%, respectively, and leading to angular errors exceeding 10° and path-fitting failures in 35% of disrupted row scenarios[15-18]. To overcome these barriers, this study introduces a multi-modal feature fusion approach. By integrating enhanced spectral analysis, advanced row-tracking algorithms, and dynamic lighting compensation, the proposed method achieves positioning accuracy within 5 cm and angular precision within ±2°. Experimental results demonstrate a significant performance boost, accelerating harvesting speed to 1.5 seconds per head and maintaining over 95% reliability in challenging conditions. Beyond cabbage, this scalable framework paves the way for automated harvesting of lettuce, Chinese cabbage, and other leafy vegetables, driving the development of versatile agricultural robotics.

2. Analysis of Agronomic Traits and Cultivation Systems for Cabbage Varieties

2.1 Comparison of Agronomic Parameters and Cultivation Patterns of Main Cultivated Varieties

Xiangcheng County, Xuchang City, Henan Province, is one of the important cabbage planting bases in China. Owing to its unique geographical environment and suitable climatic conditions, it exhibits distinct regional characteristics in cabbage cultivation. According to data from the Xiangcheng County Vegetable Planting Technical Guidelines, the local main cabbage varieties are ‘Zhonggan 192’ and ‘Zhonggan 56’, which differ in planting patterns and management practices.

ISSN: 2414-1895 DOI: 10.6919/ICJE.202506_11(6).0033

‘Zhonggan 192’ typically has a planting row spacing of approximately 80 cm and a plant spacing of 35-40 cm, with 3,000 - 3,500 plants per mu. This configuration of row and plant spacing fully considers the needs of mechanized operations, ensuring smooth passage of agricultural machinery between rows while facilitating normal growth and development of cabbage plants. The ridge height is generally 15 - 18 cm, with a slightly arched shape to facilitate rainwater drainage and prevent root waterlogging and diseases. ‘Zhonggan 192’ has a longer growth cycle, requiring approximately 60 d from transplanting to mature harvesting, with a total cycle (including the seedling stage) of about 90 d. It is mainly suitable for large-scale open-field cultivation.

‘Zhonggan 56’, an early-maturing variety suitable for dense planting to increase yield, has a row spacing of 55 - 60 cm and a plant spacing of 25 - 30 cm, with a higher planting density of 4,400 - 5,000 plants per mu. The ridge height is relatively lower (10 - 12 cm), which is conducive to shallow ridge film mulching in protected fields to maintain soil moisture and temperature. Zhonggan 56 has a shorter growth cycle, requiring about 46 d to mature after transplanting, with a total cycle of 70 - 75 d (including a 25 – 30 d seedling stage). It is typically used for greenhouse cultivation.

2.2 Cultivation Systems and Environmental Parameters of Experimental Fields.

The sampling field employed ‘Zhonggan 192’, a cabbage cultivar with a representative planting layout. With a row spacing of around 80 cm and a plant spacing of approximately 35 cm, this configuration optimally balances the need for individual plant growth, facilitating photosynthesis and nutrient uptake, while simultaneously accommodating agricultural machinery operations such as inter-tillage, fertilization, and harvesting. The ridges, measuring 15 cm in height and featuring a gentle arch, significantly improve water drainage efficiency. This hydraulic optimization minimizes the likelihood of water logging around the root zone, thereby substantially reducing the incidence of root - borne diseases. The growth cycle of this cabbage variety typically spans 60 d from transplantation to harvest. During the initial seedling phase, the plants are small with limited foliage, primarily focusing on root and leaf development. As the plants progress into the rosette stage, there is a rapid increase in leaf number and size, forming a dense, compact structure; this period is characterized by heightened requirements for light and nutrients, intensifying competition among plants. Finally, the heading stage is marked by leaves enveloping inward to form a mature head, signaling the onset of the critical harvesting period. Notably, cabbage exhibits distinct morphological and color changes throughout these developmental stages.

The cabbage cultivation environment is inherently complex, subject to multiple influential factors. In the field, issues such as missing or skipped plants frequently result in uneven plant distribution and gaps along the ridges. Moreover, weeds with similar coloration and morphology to cabbage can impede the accurate extraction of navigation lines. Fluctuations in lighting conditions, which vary significantly with time of day and weather-ranging from the soft illumination of dawn to the intense midday sun and the angled rays of dusk, also reduce the RGB contrast between cabbage leaves and soil, complicating visual segmentation. These compounding environmental variables collectively present substantial challenges to vision-based navigation systems utilized in agricultural automation.

3. Analysis of Core Algorithms

3.1 Multi-Mask Fusion Segmentation Strategy based on HSV Color Model

To address the limitations of the Excess Green (ExG) and Excess Red (ExR) Feature Grayscale methods, this study proposes a multi-mask fusion segmentation strategy based on the HSV color model, enhancing adaptability to complex scenarios through a multi-dimensional feature decoupling mechanism. This method decomposes color information into three HSV dimensions (hue, saturation, value), aligning with human perceptual characteristics and address lighting/color gradient issues.

3.1.1 Color Space Conversion and Noise Suppression

After converting images from the BGR to HSV color space, median filtering is first applied to remove salt-and-pepper noise. The nonlinear nature of a 3×3 median filter is applied to suppress salt-and-

ISSN: 2414-1895 DOI: 10.6919/ICJE.202506_11(6).0033

pepper noise points (e.g., soil specular reflections) while avoiding contour softening caused by Gaussian blur, significantly enhancing the robustness of subsequent processing.

3.1.2 Hierarchical Threshold Setting

(1) Vegetation Layer Extraction. Hue thresholds are set to cover both green leaves and yellowing core regions. Experiments show that the main hue peak of leaves concentrates within the typical green range, while the yellowing core regions in mature cabbages shift toward the yellow spectrum. The hue threshold for yellowing regions (approximately 40) remains far higher than that for soil, and expanding the lower threshold range of hue effectively reduces hole formation in yellowing cores. Additionally, hue is less affected by light intensity, enabling accurate vegetation layer extraction even under strong exposure.

(2) Plastic Mulch Detection. Although the plastic mulch layer exhibits discrete features in the hue channel and is difficult to extract, the high-reflectivity mulch is identified using the saturation and value channels. White plastic mulch shows significantly higher responses in the value channel than soil, while its low saturation further distinguishes it from soil.

(3) Interference Exclusion. Independent hue and saturation thresholds within the yellow range are set to precisely remove interference from yellow soil, withered grass, and other contaminants from the total mask.

3.1.3 Optimization and Post-Processing

Closing operations are used to fill small holes, and opening operations to smooth edge burrs, ultimately producing coherent and pure segmentation results. The combined use of closing followed by opening operations effectively fills internal holes and smooths edges in images while filling internal holes and smoothing object contours. This combination is particularly effective for processing images with complex backgrounds and noise (see Fig.1).

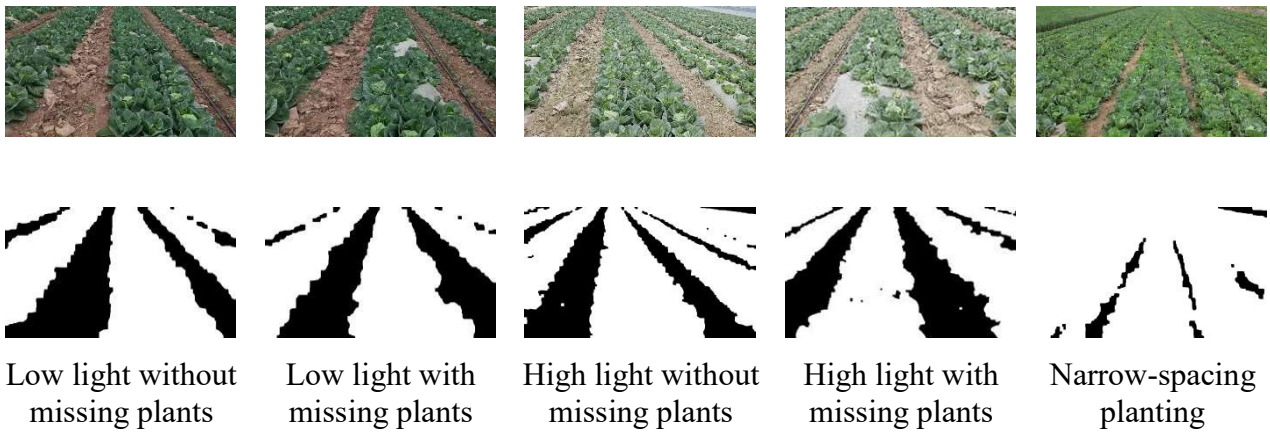

Fig. 1 Multi-Mask Fusion Segmentation Map Based on HSV Space

3.1.4 Advantage Verification

Histogram analysis reveals significant distribution differences between green vegetation and soil in the hue, saturation, and value channels (see Fig.2). Overlapping regions that are difficult to distinguish using traditional methods show clear separation in the HSV space, with almost no intersection between the hue ranges of green vegetation and soil, and the hue range remaining stable across different light intensities. Experimental results demonstrate that this method significantly outperforms the traditional ExG method in metrics such as lighting adaptability, noise resistance, and contour integrity, and also surpasses the improved ExR method under high-light-intensity conditions.

ISSN: 2414-1895 DOI: 10.6919/ICJE.202506_11(6).0033

(a)Original Image Under Low-Light Conditions

(b) Original Image Under High-Light Conditions

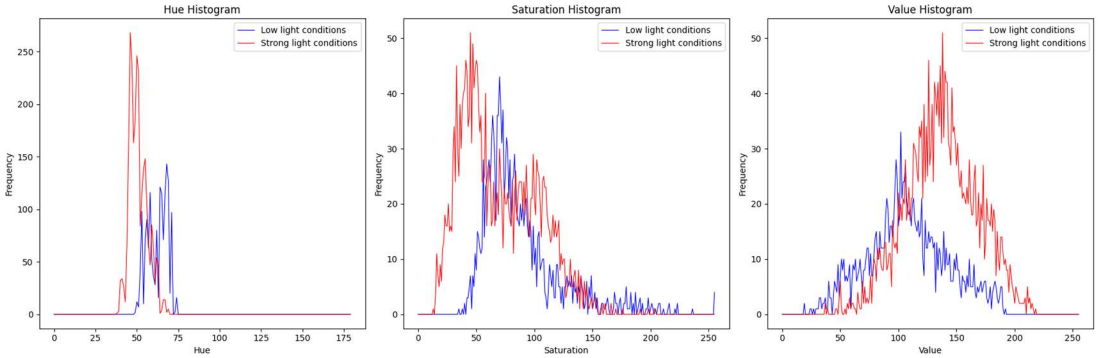

(c) HSV Histogram of Green (Cabbage)

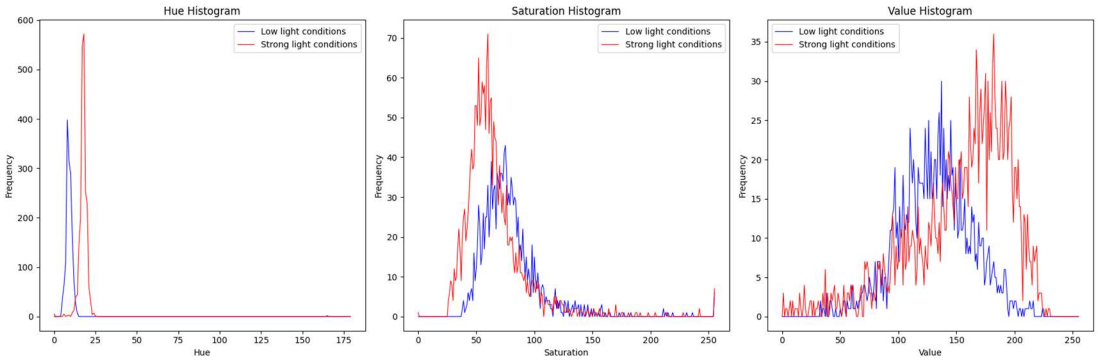

(d) HSV Histogram of Yellow (Soil)

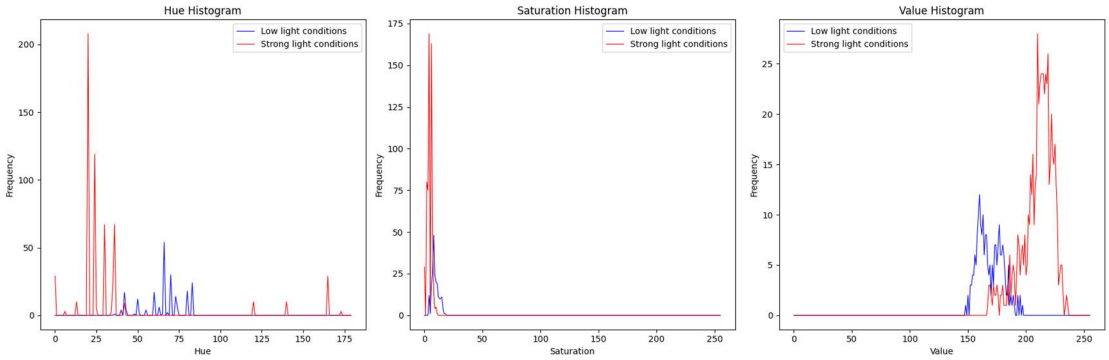

(e) HSV Histogram of White (Plastic Mulch)

Fig. 2 Histogram Comparison Based on HSV Color Space Under Different Lighting Conditions

ISSN: 2414-1895 DOI: 10.6919/ICJE.202506_11(6).0033

3.2 Navigation Boundary Line Extraction Algorithms

3.2.1 Cabbage Bilateral Navigation Line Extraction Algorithm based on Excess Green (ExG) Features

Following ExG image segmentation, a sliding window method is employed to determine the left and right edge points of cabbage plants, with least-squares fitting used to approximate these edge points as straight lines for defining bilateral navigation lines[19]. The sliding window process is as follows:

Assuming an image height of h and width of w, an $h \times w$ window is used for column-wise scanning. For each column, the number of white pixels $N(i)$ and the average white pixel count $sum(i)$ within the window are calculated.

To identify the left edge point, scanning initiates from the image center and proceeds leftward. A point i is marked as the left edge when $N(i+1)>sum(i)$ and $N(i)<sum(i)$. Similarly, for the right edge point, scanning starts from the center and moves rightward, with i marked as the right edge when $N(i+1)<sum(i)$ and $N(i)>sum(i)$.

During the mature growth stage, under conditions of missing plants or strong light, over-segmentation in image processing can cause navigation key points on both sides to shift toward the center, leading to linear fitting deviations that may result in navigation lines crushing crop edges. Additionally, in weedy fields, the sliding window method may misplace key points outward due to over-emphasis on green weed features. This indicates that traditional methods-relying on ExG-based grayscale processing, Otsu's thresholding for segmentation, and sliding window-least squares for key point selection and fitting-exhibit limitations in complex field environments (e.g., weeds, lighting variations). Such factors can cause errors in key point selection, compromising navigation line accuracy and orientation[20-22].

3.2.2 Cabbage Bilateral Navigation Line Extraction Algorithm based on Excess Green (ExG) Features

Hough transform offers unique advantages in cabbage navigation line extraction, particularly in noise handling. By transforming image space problems into parameter space and leveraging point-line duality for shape detection, it is insensitive to image noise[23]. During the cabbage heading stage, under low-light conditions, ExR grayscale combined with Otsu's thresholding produces clear image segmentation with minimal noise, allowing the Hough transform to directly and accurately locate ridge spacing and plan bilateral navigation lines.

However, the Hough transform reveals practical limitations. First, in images with multiple cabbage rows, it struggles to accurately identify bilateral navigation lines for the central row due to inherent constraints in distinguishing central rows from adjacent ones, making it susceptible to interference from other rows. Second, the Hough transform is sensitive to lighting conditions[24]. Under strong light, soil specular reflection can fragment the segmented soil region into numerous small holes, whose distorted edge points significantly affect the voting process. When holes are continuous and abundant, straight lines traversing them may accumulate higher vote counts than ideal lines, causing false detections and navigation line deviations. Missing plants further degrade performance, as inward-shifted edge points lead to severe linear fitting errors. These issues highlight that the Hough transform's robustness is insufficient for complex field environments, relying heavily on parameter adjustments that cannot effectively resist diverse interference.

3.2.3 Row-Tracking-Based Navigation Line Extraction Algorithm

Precise navigation line extraction is critical for enhancing efficiency and quality in agricultural machinery automation[25]. The proposed row-tracking algorithm addresses traditional methods' limitations in complex field environments by integrating multi-feature fusion and dynamic feedback mechanisms, improving anti-interference capability, accuracy, and efficiency. Its core workflow includes parameter initialization with historical midpoint recording, hierarchical scanning under perspective constraints, edge feature response detection, trajectory consistency verification, and robust navigation line fitting.

ISSN: 2414-1895 DOI: 10.6919/ICJE.202506_11(6).0033

(1) Parameter Initialization and Historical Midpoint Recording. The algorithm initiates with parameter initialization, creating left boundary point set P_L and right boundary point set P_R to store detected edge points, while constructing a historical midpoint queue of length N.

$$Q_m = \{m_{t-N}, \ldots\ldots m_{t-1}\} \tag{1}$$

A dynamic reference point s_t is calculated via sliding window averaging to enable adaptive adjustment of scanning start points for each pixel row.

$$s_t = \frac{1}{N}\sum_{i=1}^{N} m_{t-i} \tag{2}$$

This dynamic mechanism predicts current row positions from historical data, providing stable starting points for edge detection. It ensures continuous tracking along the target row's trajectory even in the presence of multiple rows, row curvature, or large heading angles.

(2) Hierarchical Scanning Mechanism Under Perspective Constraints. Taking the image coordinate system $I_{(x,\,y)} \in R^{480*640}$ as an example, the algorithm performs bottom-up interlaced scanning with a step size of $\delta = 4$. A scanning band width function $W(y)$ is defined.

$$W(y) = W_0 \times 0.9946^{y} \tag{3}$$

W_0 is the baseline width, and y represents the position of the current scanning row. 0.9946 is an experimental parameter adjusted for different perspective relationships. The window size decreases exponentially with increasing scanning height y, adhering to geometric constraints of perspective projection. This reduces blind search time and enables scanning windows to better follow row trajectories, improving edge point detection accuracy and long-distance scanning precision.

(3) Edge Feature Response Detection. The algorithm employs a 200*1-pixel linear detection strip to scan bidirectionally from the dynamic reference point s_t horizontally. A valid boundary is identified when the proportion of black pixels within the window exceeds 80%, with boundary point coordinates refined to the inner 1/5 position of the window. This mechanism effectively filters out hole and noise interference. By setting a reasonable pixel ratio threshold, it accurately discriminates boundaries between cabbage and soil/weeds, providing a reliable data foundation for navigation line fitting.

(4) Trajectory Consistency Verification. Upon detecting edge points, their validity is immediately verified by calculating deviations from historical points using Q_m, P_L, and P_R. Points exceeding a 10-pixel deviation threshold are discarded as false detection, while valid points are added to boundary point lists. This synchronous detection-validation mechanism forms a dynamic optimization loop, correcting detection errors in real time to reduce false positive rates and ensure boundary point accuracy and navigation line extraction stability.

(5) Robust Navigation Line Fitting. The RANSAC algorithm is used to iteratively screen inlier sets by randomly sampling 15 points to generate candidate line models M:

$$ax + by + c = 0 \tag{4}$$

The algebraic distance r_i from each point to the model is calculated, and the model with the highest inlier count ($r_i < 2$ pixels) is selected for final navigation line fitting via least squares.

ISSN: 2414-1895 DOI: 10.6919/ICJE.202506_11(6).0033

$$r_i = |ax_i + by_i + c| \quad (5)$$

This method effectively rejects outliers, ensuring global optimal line fitting based on proximal points even for slightly curved or tilted rows at distal positions, thus guaranteeing accurate and stable path guidance.

(6) Algorithm Advantages. The proposed row-tracking-based navigation line extraction algorithm offers multiple advantages: it filters interference using an 80%-pixel ratio threshold, achieves multi-row interference resistance through historical midpoint-adjusted scanning starts, and demonstrates stable performance under complex conditions such as strong light, weeds, missing plants, and large heading angles. Its perspective-adaptive window scanning reduces search time and improves efficiency, while RANSAC enhances outlier robustness to ensure navigation line accuracy. Collectively, this algorithm provides reliable navigation support for mechanized cabbage farming, with broad application prospects.

3.3 Navigation Centerline Extraction Algorithms

3.3.1 Cabbage Navigation Tracking Centerline Extraction Algorithm based on Excess Green (ExG) Features

Traditional cabbage navigation centerline extraction methods primarily rely on Excess Red (ExR) or Excess Green (ExG) feature-based grayscale processing, combined with sliding window techniques to locate left and right edges, determine navigation center points, and fit navigation lines via linear regression. Specifically, the ExG method segments images by leveraging color differences between cabbage and soil, identifies edge positions using sliding windows, calculates midpoints between left and right edges as navigation centers, and employs least-squares fitting for line regression. However, the sliding window method often misidentifies edge points in distant image regions, causing centerline deviations. Complex scenarios-such as strong lighting, weeds, missing plants, or curved rows-exacerbate this issue due to environmental interference, limiting the method's accuracy and stability in real-world fields.

3.3.2 Cabbage Navigation Tracking Centerline Extraction Algorithm based on Excess Red (ExR) Features

ExR-based algorithm proceeds was as follows: The left half of the image is selected as a sub-image to reduce data volume and focus on one side of the cabbage row for efficient edge detection. After determining the number of rows in the sub-image, each row is scanned from right to left to record the coordinate of the first pixel with a brightness value of 1, designated as the left edge point. Right edge points are identified using a symmetrical approach. Assuming distinct ExR contrast between cabbage and soil, edges are distinguished via simple brightness thresholding. Navigation center points are calculated as the arithmetic mean of left and right edge coordinates per row, with their coordinates used to construct a center point cloud for least-squares linear fitting.

This algorithm has notable limitations: First, its single-point brightness-based edge detection lacks validation, making it highly sensitive to segmentation quality, noise, and lighting variations. Second, unfiltered outlier points in least-squares fitting reduce detection success and precision under complex or high-light conditions. Additionally, fixed starting points for scanning limit heading angle adaptability, failing to handle curved or tilted rows. Collectively, these factors compromise its robustness and accuracy in practical applications.

3.3.3 Intersection Bisector-Based Cabbage Navigation Centerline Extraction Algorithm

In cabbage planting navigation, centerline extraction accuracy is critical for machinery efficiency and operation quality. The proposed intersection bisector-based algorithm achieves stable centerline extraction through precise geometric calculations and vector analysis, comprising three key steps: boundary line intersection modeling, direction vector synthesis and normalization, and centerline parameter resolution.

ISSN: 2414-1895 DOI: 10.6919/ICJE.202506_11(6).0033

(1) Boundary Line Intersection Modeling

Let the left and right navigation boundary lines be defined as $L_1 = k_1 y + b_1$ and the right navigation boundary line be $L_r = k_2 y + b_2$. The intersection point (x_v, y_v) of these two lines is calculated by solving their simultaneous equations:

$$\begin{cases} y_v = \dfrac{b_2 - b_1}{k_2 - k_1} \\ x_v = k_1 y_v + b_1 \end{cases} \tag{6}$$

When $k_1 = k_2$, an exception handling mechanism is triggered, and historical trajectory interpolation is used for compensation.

(2) Direction Vector Synthesis and Normalization

A sampling point $y_s = y_v + 1$ (1 pixel below the intersection) is set to calculate projection points x_l and x_r on the left and right navigation boundary lines at this position. The direction vectors V_l and V_r of the left and right navigation lines are constructed and normalized as follows:

$$\begin{cases} V_l = \dfrac{(x_l - x_v, y_s - y_v)}{\left|(x_l - x_v, y_s - y_v)\right|} \\ V_r = \dfrac{(x_r - x_v, y_s - y_v)}{\left|(x_r - x_v, y_s - y_v)\right|} \end{cases} \tag{7}$$

The direction of the angle bisector is obtained through vector synthesis:

$$V_c = V_l + V_r \tag{8}$$

(3) Centerline Parameter Resolution

Based on the synthesized direction vector V_c of the angle bisector, with components V_{cx} and V_{cy}, the slope of the centerline is calculated as:

$$k_c = \frac{V_c[x]}{V_c[y]} \tag{9}$$

The centerline equation is established as:

$$x = k_c (y - y_v) + x_v \tag{10}$$

This process satisfies the geometric constraint of the angle bisector theorem (equal distances from points to both side boundaries), ensuring the centerline lies between the left and right navigation lines with a reasonable direction.

(4) Navigation Line Extraction Demonstration

By accurately solving boundary line intersections and using vector synthesis for bisector direction determination, the algorithm ensures the centerline remains geometrically valid between

ISSN: 2414-1895 DOI: 10.6919/ICJE.202506_11(6).0033

boundaries(see Fig.3 and Fig.4). Experiments show stable and precise centerline extraction under complex conditions (e.g., lighting variations, weed interference), providing reliable path guidance for mature cabbage harvesting machinery. Leveraging the geometric relationship between boundary lines, this method enhances centerline extraction accuracy and stability, making it suitable for real-world agricultural applications.

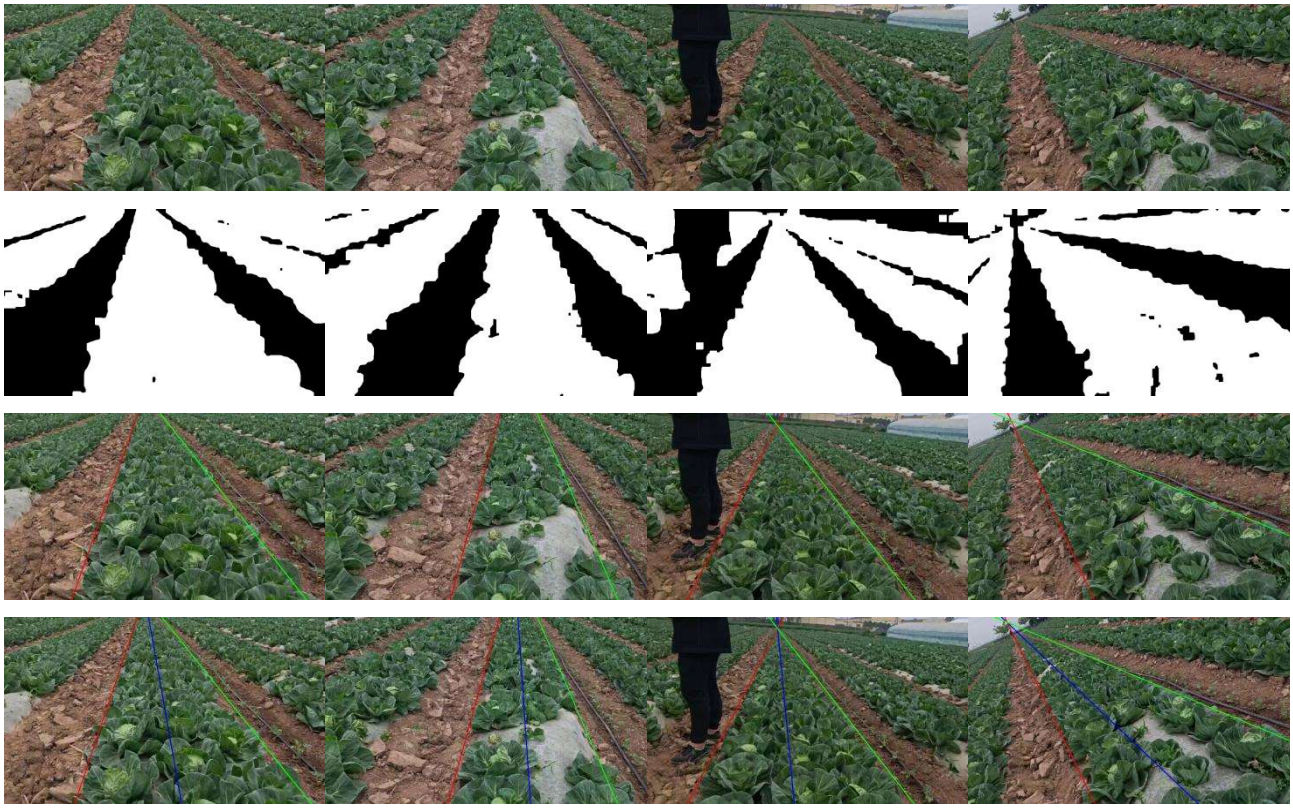

(a)No missing plants (b)Missing plants (c)Complex background interference (d)Large heading angle

Fig. 3 Navigation Line Extraction Effects in Different Scenarios Under Low-Light Conditions

ISSN: 2414-1895 DOI: 10.6919/ICJE.202506_11(6).0033

(a)No missing plants (b)Missing plants (c)Complex background interference (d)Large heading angle

Fig. 4 Comparison of Navigation Line Extraction Effects in Different Scenarios Under High Light

4. VarietiesExperiments and Discussion

4.1 Image Acquisition

Image acquisition forms the foundation of this study, directly impacting the performance of subsequent navigation line extraction algorithms and the final harvesting outcomes. The OmniVision OVH9000 camera, featuring 4x low-light sensitivity, was selected to ensure clear image capture even in dim conditions.

The acquisition protocol was meticulously designed to align with cabbage planting patterns and operational environments. The camera was positioned slightly above and directly facing the cabbage plants to capture crown features and inter-row structures distinctly. An optimal working distance of 1.5 meters from the plants was maintained, balancing image resolution with the need to cover sufficient inter-row context.

Data were collected during two critical periods: 11:00 - 14:00 for high-light conditions and 16:00 - 18:00 for low-light scenarios, covering the full range of natural illumination. Field experiments were carried out in Xiangcheng County, Xuchang, Henan Province, using ‘Zhonggan 56’, a locally representative cabbage variety. Each dataset incorporated variations in weed presence or absence, plant density (normal or with missing plants), camera tilt to simulate different heading angles, and complex background interference. These scenarios mimic real-world challenges to enhance algorithm adaptability. Images were captured at a resolution of 640×480 pixels to optimize the trade-off between quality and computational efficiency. Operators followed a predefined grid pattern, regularly verifying image integrity to ensure clear cabbage features and unobstructed inter-row views. In challenging conditions (e.g., weedy plots, missing plants), shooting angles were adjusted to accurately represent field variability.

4.2 Data Annotation

Manual annotation was employed to precisely delineate navigation lines[26]. Experts traced bilateral boundary lines along row edges and marked the central navigation line, creating ground-truth references for algorithm evaluation. Each annotated image contained three critical lines, serving as benchmarks for validating extraction results. The dataset comprised 3259 images divided into two subsets: 1116 high-light and 2143 low-light images, providing ample data for robust performance assessment.

4.3 Results Analysis

Using 3259 annotated images across varying lighting conditions, navigation line planning for heading-stage cabbages was conducted on a test system equipped with an Intel i7 processor and PyCharm 2023.3.4. Visualizations demonstrate the proposed method's effectiveness in generating navigation lines for diverse scenarios. Quantitative evaluations in Table 1 and Table 2 confirm superior performance in navigation accuracy, orientation precision, and robustness compared to baseline methods.

ISSN: 2414-1895 DOI: 10.6919/ICJE.202506_11(6).0033

Table 1. Comparison of Average Navigation Line Angle Difference and Time Consumption

Algorithm	Left and Right Navigation Tracking Lines			Central Navigation Line	
	Average Time Consumption /s	Average Angle Difference of Left Navigation Line/ (°)	Average Angle Difference of Right Navigation Line/ (°)	Average Time Consumption /s	Average Absolute Angle Difference / (°)
Row-Tracking Navigation Line Extraction Algorithm	0.192	0.291	0.259	0.001	0.240
Over-Red Feature Grayscale Method	0.086	5.710	8.300	0.420	3.260
Over-Green Feature Grayscale Method	0.210	12.860	13.250	0.228	6.760

Table 2. Comparison of Average Navigation Line Angle Differences Under Different Light Intensities

Dataset	Number of Images (sheets)	Left and Right Navigation Tracking Lines		Central Navigation Line
		Average Angle Difference of Left Navigation Line/ (°)	Average Angle Difference of Right Navigation Line/ (°)	Average Absolute Angle Difference / (°)
Dataset 1 (High Light Intensity Group)	1116	0.37	0.18	0.24
Dataset 2 (Low Light Intensity Group)	2143	0.25	0.30	0.24

5. Conclusion

This study focuses on navigation line detection algorithms for mature heading-stage cabbage, achieving notable results: the average angular difference of central navigation lines across varying lighting and environmental conditions is 0.24°, with an average boundary line extraction time of 0.192 seconds and centerline fitting time below 0.001 seconds. Key innovations include a multi-mask fusion segmentation strategy based on the HSV color model to improve navigation mask quality by accurately extracting cabbage vegetation and plastic mulch while eliminating interference; a novel row-tracking-based navigation line extraction algorithm that optimizes processes from parameter initialization to robust line fitting, enhancing accuracy and adaptability to complex scenarios; and a stable and precise centerline extraction algorithm that provides reliable path guidance for mechanized harvesting. Collectively, these advancements offer strong technical support for automated navigation in cabbage harvesting machinery, promoting agricultural automation, reducing production costs, and improving operational efficiency. For future development, refinements will focus on algorithm optimization via advanced hardware and parallel computing to enhance real-time performance,

ISSN: 2414-1895 DOI: 10.6919/ICJE.202506_11(6).0033

expanding model generalization to other leafy vegetables like Chinese cabbage and lettuce, and integrating deep learning, UAV remote sensing, and GIS data to enable large-scale planting area monitoring and intelligent path planning. Increased field trials and industry-academia-research collaboration will accelerate technology transfer, aiming to elevate navigation capabilities for cabbage harvesting robots, drive agricultural cost-efficiency, and foster the intelligentization of modern farming toward high-precision, efficient, and automated agricultural production.

Acknowledgments

This research was supported by the 2024 Science and Technology Key Project of Henan Province (Grant No. 242102111181), Open Project of Key Laboratory of on Site Processing Equipment for Agricultural Products, Ministry of Agriculture and Rural Affairs of China, and the Special Project for High-Level Talents of Henan Agricultural University (Grant No. 30501572). The authors extend sincere gratitude to the faculty members and administrative teams at both institutions for their invaluable guidance and logistical support.

References

[1] Bai Y, Zhang B, Xu N, Zhou J, Shi J, Diao Z. Vision-based navigation and guidance for agricultural autonomous vehicles and robots: A review[J]. Computers and Electronics in Agriculture, 2023, 205: 107584.

[2] Gao S, Yang K, Shi H, Wang K, Bai J. Review on Panoramic Imaging and Its Applications in Scene Understanding[J]. IEEE Transactions on Instrumentation and Measurement, 2022, 71: 1–34.

[3] He Jing, Zang Y, Luo X, Zhao R, He Jie, Jiao J, Key Laboratory of Key Technology on Agricultural Machine and Equipment, Ministry of Education, South China Agricultural University, Guangzhou 510642, China. Visual detection of rice rows based on Bayesian decision theory and robust regression least squares method[J]. International Journal of Agricultural and Biological Engineering, 2021, 14(1): 199–206.

[4] He Y, Zhang X, Zhang Z, Fang H. Automated detection of boundary line in paddy field using MobileV2-UNet and RANSAC[J]. Computers and Electronics in Agriculture, 2022, 194: 106697.

[5] Huang P, Zhu L, Zhang Z, Yang C. Row End Detection and Headland Turning Control for an Autonomous Banana-Picking Robot[J]. Machines, 2021, 9(5): 103.

[6] Jiang P, Ergu D, Liu F, Cai Y, Ma B. A Review of Yolo Algorithm Developments[J]. Procedia Computer Science, 2022, 199: 1066–1073.

[7] Jiang Q, Wang Y, Chen J, Wang J, Wei Z, He Z. Optimizing the working performance of a pollination machine for hybrid rice[J]. Computers and Electronics in Agriculture, 2021, 187: 106282.

[8] Kaur A, Kumar M, Jindal M K. Shi-Tomasi corner detector for cattle identification from muzzle print image pattern[J]. Ecological Informatics, 2022, 68: 101549.

[9] Liu Y, Zhang Yao, Wang Y, Hou F, Yuan J, Tian J, Zhang Yang, Shi Z, Fan J, He Z. A Survey of Visual Transformers[Z]. arXiv, 2022(2022-12-06).

[10] Liu Z, Lin Y, Cao Y, Hu H, Wei Y, Zhang Z, Lin S, Guo B. Swin Transformer: Hierarchical Vision Transformer using Shifted Windows[Z]. arXiv, 2021(2021-08-17).

[11] Ma Z, Yin C, Du X, Zhao L, Lin L, Zhang G, Wu C. Rice row tracking control of crawler tractor based on the satellite and visual integrated navigation[J]. Computers and Electronics in Agriculture, 2022, 197: 106935.

[12] Mazzia V, Salvetti F, Aghi D, Chiaberge M. DeepWay: A Deep Learning waypoint estimator for global path generation[J]. Computers and Electronics in Agriculture, 2021, 184: 106091.

[13] Rabab S, Badenhorst P, Chen Y-P P, Daetwyler H D. A template-free machine vision-based crop row detection algorithm[J]. Precision Agriculture, 2021, 22(1): 124–153.

[14] Saleem M H, Potgieter J, Arif K M. Automation in Agriculture by Machine and Deep Learning Techniques: A Review of Recent Developments[J]. Precision Agriculture, 2021, 22(6): 2053–2091.

[15] Sun Q, Zhang R, Chen L, Zhang L, Zhang H, Zhao C. Semantic segmentation and path planning for orchards based on UAV images[J]. Computers and Electronics in Agriculture, 2022, 200: 107222.

ISSN: 2414-1895 DOI: 10.6919/ICJE.202506_11(6).0033

[16] Wang S, Yu S, Zhang W, Wang X, Li J. The seedling line extraction of automatic weeding machinery in paddy field[J]. Computers and Electronics in Agriculture, 2023, 205: 107648.

[17] Wang S, Zhang W, Wang X, Yu S. Recognition of rice seedling rows based on row vector grid classification[J]. Computers and Electronics in Agriculture, 2021, 190: 106454.

[18] Wang T, Chen B, Zhang Z, Li H, Zhang M. Applications of machine vision in agricultural robot navigation: A review[J]. Computers and Electronics in Agriculture, 2022, 198: 107085.

[19] Winterhalter W, Fleckenstein F, Dornhege C, Burgard W. Localization for precision navigation in agricultural fields-Beyond crop row following[J]. Journal of Field Robotics, 2021, 38(3): 429–451.

[20] Wu T, Tang S, Zhang R, Cao J, Zhang Y. CGNet: A Light-Weight Context Guided Network for Semantic Segmentation[J]. IEEE Transactions on Image Processing, 2021, 30: 1169–1179.

[21] Xue J L, Grift T E. Agricultural Robot Turning in the Headland of Corn Fields[J]. Applied Mechanics and Materials, 2011, 63–64: 780–784.

[22] Yang Y, Zhou Y, Yue X, Zhang G, Wen X, Ma B, Xu L, Chen L. Real-time detection of crop rows in maize fields based on autonomous extraction of ROI[J]. Expert Systems with Applications, 2023, 213: 118826.

[23] Yasuda Y D V, Martins L E G, Cappabianco F A M. Autonomous Visual Navigation for Mobile Robots: A Systematic Literature Review[J]. ACM Computing Surveys, 2021, 53(1): 1–34.

[24] Yu C, Gao C, Wang J, Yu G, Shen C, Sang N. BiSeNet V2: Bilateral Network with Guided Aggregation for Real-Time Semantic Segmentation[J]. International Journal of Computer Vision, 2021, 129(11): 3051–3068.

[25] Yu Y, Bao Y, Wang J, Chu H, Zhao N, He Y, Liu Y. Crop Row Segmentation and Detection in Paddy Fields Based on Treble-Classification Otsu and Double-Dimensional Clustering Method[J]. Remote Sensing, 2021, 13(5): 901.

[26] Zheng S, Lu J, Zhao H, Zhu X, Luo Z, Wang Y, Fu Y, Feng J, Xiang T, Torr P H S, Zhang L. Rethinking Semantic Segmentation from a Sequence-to-Sequence Perspective with Transformers[Z]. arXiv, 2021(2021-07-25).